Molecular Crystals and Liquid Crystals Science and Technology. Section A. Molecular Crystals and Liquid Crystals

Publication details, including instructions for authors and subscription information:
http://www.tandfonline.com/loi/gmcl19

Thermal Study of an Antiferroelectric Liquid Crystal

J. A. Puértolas [a] , M. Castro [a] , M. R. De La Fuente [b] , M. A. Pérez Jubindo [b] , H. Dreyfus [c] , D. Guillon [c] & Y. González [d]

[a] Dpto. Ciencia de Materiales. Centro Politécnico Superior-ICMA. Universidad deZaragoza-C.S.I.C., 50015, ZARAGOZA, Spain

[b] Dpto. Fisica Aplicada II. Facultad de Ciencias. Universidad del Pais Vasco, 48080, BILBAO, Spain

[c] Institut de Physique et Chimie des Matériaux de Strasbourg, CNRS-UL P-EHICS., 67037, Strasbourg-Cedex, France

[d] Dpto. Química Organica. Facultad de Ciencias-ICMA Universidad de Zaragoza-CSIC, 50009, ZARAGOZA, Spain

Version of record first published: 24 Sep 2006.

Mol. Cryst. Liq. Cryst., 1996, Vol. 287, pp. 69–82
Reprints available directly from the publisher
Photocopying permitted by license only

Thermal Study of an Antiferroelectric Liquid Crystal

J. A. PUÉRTOLAS[a], M. CASTRO[a], M. R. DE LA FUENTE[b], M. A. PÉREZ JUBINDO[b], H. DREYFUS[c], D. GUILLON[c] and Y. GONZÁLEZ[d]

[a]*Dpto. Ciencia de Materiales. Centro Politécnico Superior-ICMA. Universidad de Zaragoza-C.S.I.C., 50015 ZARAGOZA (Spain)*

[b]*Dpto. Física Aplicada II. Facultad de Ciencias. Universidad del Pais Vasco 48080 BIL BAO (Spain)*

[c]*Institut de Physique et Chimie des Matériaux de Strasbourg. CNRS-UL P-EHICS. 67037 Strasbourg-Cedex (France)*

[d]*Dpto. Química Organica. Facultad de Ciencias-ICMA Universidad de Zaragoza-CSIC, 50009 ZARAGOZA (Spain)*

(Received August 21, 1995; in final form January 12, 1996)

A full thermal study of the antiferroelectric liquid crystal (R)-1-methylheptyl 4'-(4''-decyloxybenzoyloxy)-biphenyl-4-carboxylate (MHDOBBC) has been carried out by high resolution ac calorimetry, DSC and the analysis of the implemented and denoted "thermistor method". The melting and the freezing transitions of Sc^*_A have been studied using the latter method, with regard to pre-transitional effects, conversion rates, metastability and latent heat ratio. A new monotropic phase has been detected following investigations by ac calorimetry, X-rays, dielectric measurements and optical observation and its possible identity is discussed. The S_A-S_C* transition is well described by the extended Landau model and a comparative analysis is performed with the related compounds MHPOBC and MHPOCBC. No clear evidence of phase restructuring appears in ac calorimetry and DSC measurements, except for an anomaly close to the $Sc^*\gamma$-Sc^*_A transition.

Keywords: Antiferroelectric, liquid crystal, AC calorimetry.

1. INTRODUCTION

The study of antiferroelectricity in liquid crystals is one of the most fascinating current research topics in this subject due to the variety of new smectic subphases present in the temperature region throughout S_A/S_{CA}^* phases, e.g. $S^*_{C\alpha}$, S_C*, $S_{C\gamma}^*$. These intermediate ferrielectric and antiferroelectric configurations, which constitute a Devil's staircase, are a consequence of the competition between the pairing energy of the transverse dipole moments in neighboring layers stabilizing the S_{CA}^* phase, and the packing energy in the S_C^* phase. On the other hand, technical applications of the antiferroelectric smectic phases, like flat panel displays using tristable switching for multiplex driving, make them very attractive. References to all these scientific and technical features appear in a recent review by Fukuda *et al*[1].

Thermal studies, which have been carried out in order to clarify the successive subphases, determine their transition character and study the metastability and the

freezing process of the antiferroelectric phases. Several measurements using different thermal techniques have focused on the antiferroelectric liquid crystal 4-(1-methylheptyloxycarbonyl)-phenyl4′-octyloxy-biphenyl-4-carboxylate(MHPOBC). DSC measurements allowed all the transitions to be distinguished without determining the extremely small enthalpy changes[2]. Modulated calorimetry was used by Chandani with success only the S_A-$S^*_{C\alpha}$ transition[2]. The restructuring transitions were observed through a relaxation method by Ema *et al*[3]. Adiabatic calorimetry measurements also show all these transitions[4]. Finally, Kim has correlated the thermodynamic properties observed by DSC with the conformation changes in the compound detected by Raman scattering and X-ray diffraction[5]. In other related compounds, we can mention the complete analysis of the kinetic freezing of the S^*_{CA} phase in the MHPOCBC (the octyloxy tail group of MHPOBC is replaced by an octanoyl group) using ac calorimetry[3], and the Neundorf study on the polymorphism of the R-1-methylheptyl-4-(4′-n-octyloxybiphenyl-4-yl-oxymethylene) benzoate (MHOBMB) compound by means of DSC, thermal expansion coefficient and X-ray measurements[6].

However, few studies have been performed on the antiferroelectric liquid crystal (R)-(S)-1-methylalkyl 4′(4″-alkoxybenzoyloxy)biphenyl-4-carboxylate family[7-8], synthesized by Goodby[9], and where the biphenyl group is close to the chiral group. From this family, we have chosen the compound (R)-1-methylheptyl 4′-(4″-decyloxybenzoyloxy) biphenyl-4-carboxylate (hereafter abbreviated as MHDOBBC), since it belongs to the two series in

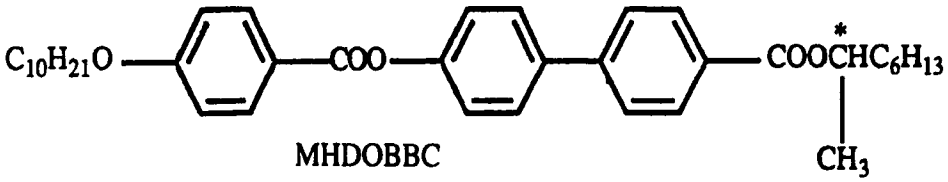

MHDOBBC

STRUCTURE 1

which the antiferroelectric properties are studied as a function of peripheral alkyl chain length. On the other hand, the MHDOBBC compound presents the lowest values of the S^*_{CA}-S^*_J and recrystalization transition temperatures, within the alkoxy chain series. On cooling, the phase transition sequence is: I-397.6 K-S_A-378.0 K-S_C*-350.7 K-$S_{C\gamma}$*-345.2 K-S^*_{CA}-320.6 K-S_J*-289 K-Crystal[9].

The aim of this work is to perform a complete thermal study of MHDOBBC, which involves the region of phase restructuring the S_A-S^*_C transition and the complex freezing behaviour of the S^*_{CA} phase. For the latter study we have used a new thermal method denoted as "thermistor method", which will be briefly explained in this paper.

2. EXPERIMENTAL

2.1. Techniques

Specific heat measurements on the antiferroelectric (R)-1-methylheptyl 4'-(4"-n-decyloxybenzoyloxy) biphenyl-4-carboxylate have been performed using a high-resolution ($\pm 0.1\%$) and automatically controlled ac calorimeter, which has been described elsewhere[10]. Here we will review its essential features.

The source of the modulated input power is a strain gauge which operates as a resistive heater and as the sample support. A microbead thermistor, supplied by a high stabilized home-built dc current supply, allows the detection of the temperature oscillations of the sample. A lock-in amplifier (EG&G PAR 5302) acts as an oscillator for the heater and also measures the ac voltage and phase shift generated in the thermistor. The dc temperature of the sample is determined from the sampling of the thermistor voltage in some periods with a HP3457A digital voltmeter. For our compound, MHDOBBC, the sample holder was a commercial aluminium capsule used in DSC measurements, with a volume of 10 μl and containing 23 mg of sample. The sample holder is surrounded by two concentric copper blocks and immersed into a thermostatic bath (Lauda KP20D model). The temperature controller of the bath allows the temperature to be scanned with different rates from 0.2 to 5 Kh^{-1}. The block temperature is measured with a Fluke 8840A multimeter, using a calibrated platinum thermometer as sensor.

A frequency sweep between 8 mHz to 100 mHz at room temperature has been carried out in order to select the operating frequency, 15 mHz, where a linearity between the inverse of the ac signal and the specific heat was obtained. The sample temperature oscillations at room temperature, in the region outside the transitions, were around 30 mK and the input power was 2.6 mW. The helium pressure in the internal chamber was 8 kPa.

X-ray diffraction studies were carried out with a Guinier-type focusing camera equipped with a bent quartz monochromator ($\lambda K_{\alpha 1} = 1.54056$ Å) and using an INSTED hot-stage (± 0.01°C) as a sample holder. Powder patterns (samples in 1 mm diameter Lindemann capillaries) were recorded with an INEL curved, position-sensitive detector (exposure time: 30 min) controlled by a multichannel analyzer. Experiments were conducted by a stepwise cooling of the sample (temperature steps of 0.2 °C) from the S^*_{CA} to the S_J^* phase.

The cell for the dielectric studies was made of two ITO-coated glass plates separated by 60 μm spacers. They were treated with nylons to achieve planar alignment. Temperature and dielectric measurements were fully computer controlled. Measurements have been performed on heating and on cooling at a rate of 0.5 °C min^{-1}. The dielectric permittivity has been measured with the HP4192A impedance analyzer.

2.2. Thermistor method

We have developed an alternative method to study the character of the transition compared with the usual phase shift detection in the ac calorimetric technique. The procedure is the following. When a linear temperature heating or cooling ramp is

programmed for the bath, the thermistor temperature should follows this linear scan over the whole temperature range. However, when the sample passes through a first-order transition, the latent heat absorbed or released by the sample induces a thermal variation in the temperature thermistor.

The evaluation of this thermal deviation from its practically expected linear behaviour is the basis of the method. We calculate the expected thermistor temperature in the transition region, interpolating the polynomial fit of the thermistor temperature in two temperature ranges away from the transition (below and above). The difference between the measured sample temperature (T_t) and the interpolated temperature value (T_1), taken at the same time, is denoted by $\Delta T = T_t - T_1$, which is plotted against the expected sample temperature (ΔT vs T_1). This type of representation excludes the bath temperature oscillations (± 0.005 K at 343 K in the best case), which are higher than the thermistor ones, due to the loss damping obtained with the vacuum surrounding the inner copper block.

A value of $\Delta T \neq 0$ means that some latent heat exists in the transition and that a first-order character can be assigned. In a second-order transition, no other effect has been detected due to the absence of latent heat. The high sensitivity of the thermistor and its good thermal contact with the sample holder allows the detection of small latent heats. From a rough analysis, ΔT is also related to the conversion rate of the sample at the transition. When the conversion rates are similar in different transitions, a qualitative comparison between the latent heats can be performed. More details of this method have been described elsewhere[11].

2.3. Synthesis

The MHDOBBC was synthesized using commercially available (S)-(+)-2-octanol (Aldrich) which served as enantiomerically enriched starting material. The esterification reaction was carried out following the procedure described by Mitsunobu[19]. The final and intermediate products were purified by flash-chromatography over silica gel using a mixture of hexane/dichloromethane as elunt in different proportions. Purities of the target materials were checked by thin layer chromatography. The chemical structure of all materials were analysed by 1H-NMR spectroscopy (Varian Unity-300 Bruker ARX-300) and elemental analysis (microanalysis Perkin-Elmer 2400). For the final product a mass spectral analysis (spectometer VG AutoSpec) was carried out. All the results are described in Ref. [20].

3. RESULTS AND DISCUSSION

The total heat capacity, Cp, (sample plus addenda) from 315 K to 400 K has been plotted in Figure 1. This heating run was performed at a scan rate of 1 Kh^{-1} up to 390 K and faster through the clearing transition. Three anomalies can be clearly observed, which correspond to the melting point, $T_m = 338.75$ K, the S_C^*-S_A, $T_{C^*A} = 376.50$ K and the S_A-I, $T_{AI} = 396.27$ K transitions, in accordance with those reported based on DSC measurements[9]. On cooling the sample from the isotropic phase at the same scan rate, the only noteworthy changes appear below the melting temperature, T_m, as we show in Figure 3. A monotropic crystalline phase, denoted as

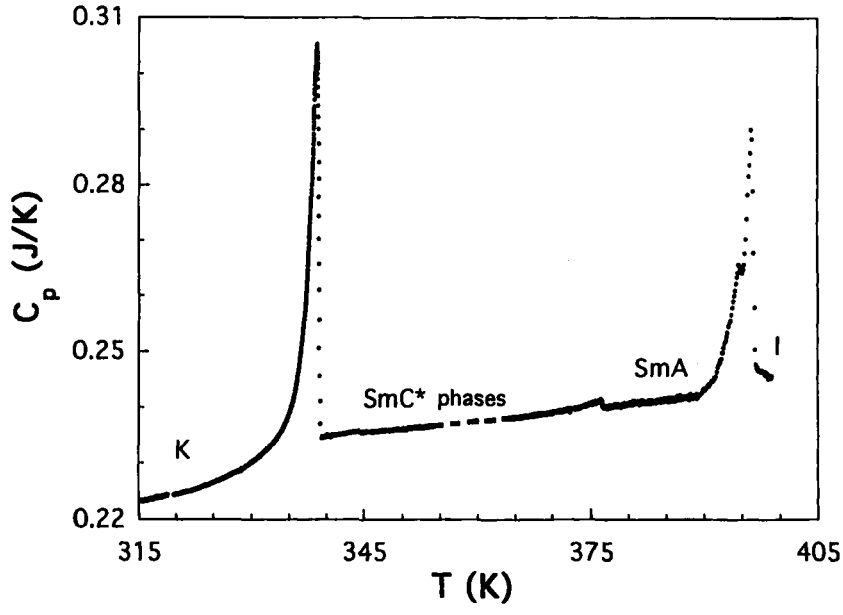

FIGURE 1 Heat capacity (sample plus addenda) measured in the ac mode at 15 mHz and with a heating rate of 1 Kh^{-1}.

S_J^* in Ref. [9] appears at 319.82 K, due to the S_{CA}^* phase freezing. A further conversion to a crystal phase occurs around 315.8 K, which will be called the K phase in this paper. An analysis of the latter results and the data obtained using other thermal scan rates will allow us to study in depth some features of the thermal behavior of this compound.

3.1. Melting and freezing transitions

In this section we will show that the "thermistor method" is an interesting tool to complete the analysis of Cp data in these first-order transitions, relative to the pre-transitional effects, conversion rates, metastability and latent heat ratio.

The melting transition, K-S_{CA}^*, shows an abrupt and extended Cp spike at 338.75 K. Since the method is sensitive to the latent heat, it will allow the definition of the limits between the regions where two phases coexist and where pre-transitional effects occur. We have obtained ΔT in this transition fitting in the temperature regions 312–324 K and 340.5–341 K and interpoling for calculating the expected background linear rate. A plot of ΔT vs T is shown in Figure 3. The vertical arrows point out the temperature range (~ 2 K) where the K phase and the S_{CA}^* phases coexist. Therefore, the rest of the region where an excess of heat capacity is observed corresponds to the pre-transitional or fluctuation region. This behaviour is similar to the one observed in the melting transition of MHPOCBC.

On cooling, a monotropic phase, S_J^* appears at 319.82 K due to freezing of the S_{CA}^* phase. The former phase extends over a small temperature range, where the heat capacity is almost constant (Figure 3). A further stepwise behaviour corresponding to

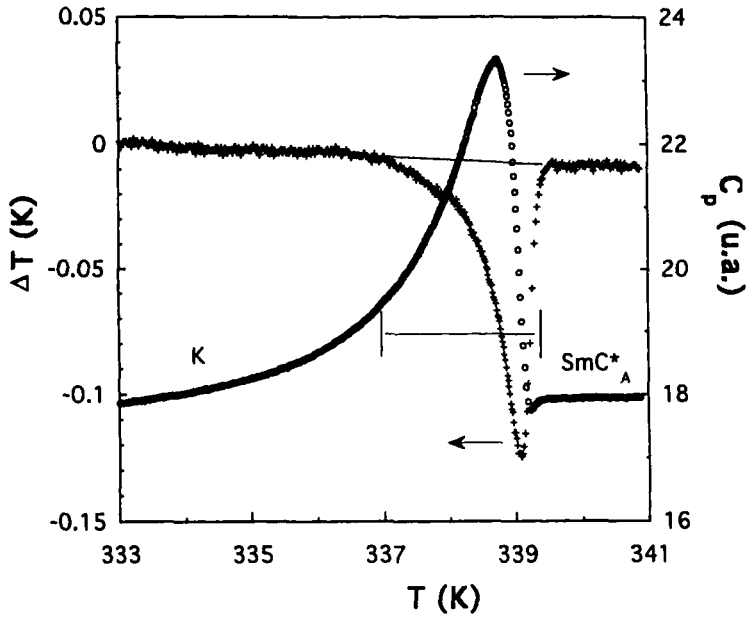

FIGURE 2 (o) Enlarged view of the peak at the melting transition obtained at 1 Kh^{-1}. (+) Plot ΔT versus T calculated with the thermistor method at this transition. The delimited region represents the two-phase coexistence region, in which the thermistor undergoes cooling.

the recrystallization transition is observed to start at 315.8 K, and to finish at 312 K. An almost negligible exothermic peak at ~ 310 K appears in our DSC curves obtained at 5 K min^{-1}. These transition temperatures are very far from the one refered to by Goodby, 289 K,[9] in spite of the fact that a strong thermal hysteresis is associated with this transition.

In Figure 3 we have also plotted ΔT vs T for this cooling process. At lower temperatures, we can observe a peak related to the S_J^*-K transition, which expands approximately in a range of six degrees. At higher temperatures, a double peak can be seen. The lowest temperature peak appears in an interval of two degrees and corresponds to the region where the S_{CA}^* converts to S_J^*. Therefore, the two crystallization transitions are also reflected in ΔT. Since the cooling rate used through the transitions was the same, $1 Kh^{-1}$, we can deduce that the rate of the crystallization process for the S_J^* phase is slower than the freezing of S_{CA}^* and therefore, that it is difficult obtain the K phase without passing through the S_J^* phase.

Concerning the highest temperature peak, we can realize that it appears in a region prior to the begining of recrystallization of the S_{CA}^* phase, where the Cp is almost constant. The only explanation for this peak should be that freezing occurs during the S_{CA}^* phase cooling process, as happens in MHPOCBC, although here the supercooling range, 18.7 K, is larger than for MHPOCBC. In order to confirm the last feature, some quench-and-hold experiments have also been carried out. The sample was cooled rapidly from a temperature higher than the melting point and then held at approximately constant temperature, 320.6 K, for a long time. After 18 h, the heat capacity

undergoes a drop to reach the values corresponding to the K phase, evidencing that the S^*_{CA} phase is a long-term metastable phase with respect to freezing. Therefore the "thermistor method" also allows the direct detection of the partial conversion of the S^*_{CA} into the K phase, not noticeable in Cp without the quench-and-hold process.

Finally, we have checked the method quantitatively. We have chosen the freezing of S^*_{CA} and the melting process for comparing latent heats, since both present a similar conversion rate. The temperature range in which $\Delta T \neq 0$ is the same, having been obtained with the same scan rates. The maximum values of ΔT are quite different, $\Delta T_{max} = 0.017\,K$ and $\Delta T_{max} = 0.12\,K$, respectively, with a value ratio of 0.14. The enthalpy values determined by DSC for these transitions are $\Delta H = 4.2\,kJ\,mol^{-1}$ and $31.7\,kJ\,mol^{-1}$, respectively[9]. The ΔH ratio is 0.13, practically equal to the ΔT_{max} ratio. Therefore, the method can also give information about latent heat, (not in an absolute way) whenever the transitions have been scanned over with the same rates and the conversion rates of the phases are similar, like the transitions analyzed here.

3.2. The New Metastable phase

The detailed view of the heat capacity peak around 320 K in the freezing S^*_{CA} process shows a shape with an internal structure similar at two overlapped peaks. In order to verify the reproducibility of these results, additional cooling runs were made at constant scan rates of 0.5 and $2\,Kh^{-1}$. Both rates verify the double structure found, and the shape of the peaks practically remain unchanged (see Fig. 4). We could therefore

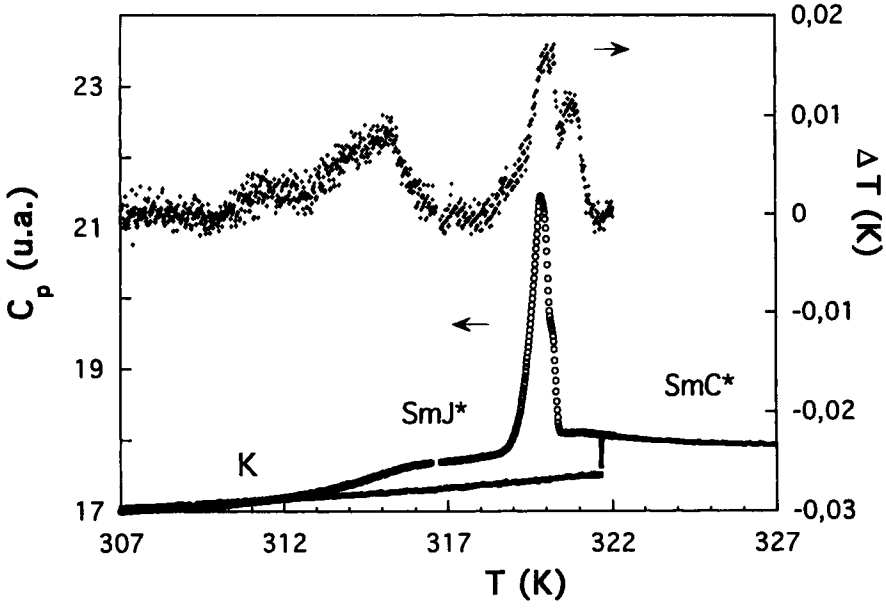

FIGURE 3 (o) Heat capacity measured at the cooling rate of $-1\,Kh^{-1}$. (+) Difference, ΔT, between the thermistor temperature and the extrapolated linear expected behaviour obtained following the method explained in the text (thermistor method).

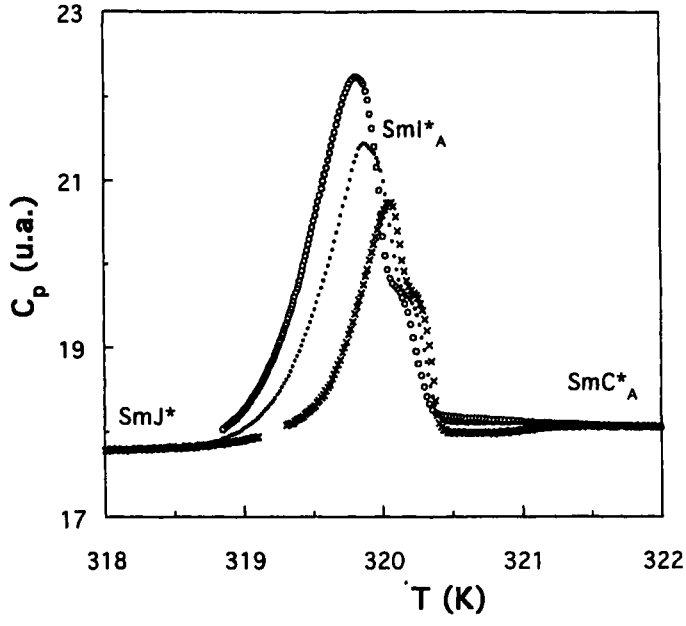

FIGURE 4 Heat capacity measured at three different cooling scan rates from S^*_{CA} phase. (x) $-0.5\ Kh^{-1}$, (•) $-1\ Kh^{-1}$, (o) $-2\ Kh^{-1}$.

consider the presence of a new phase in a narrow temperature range between the S^*_{CA} and the S^*_J.

The comparison with the thermal behaviour of other antiferroelectric compounds, like MHPOBC or MHPOCBC, can perhaps help in understanding this complex behaviour. So, in both compounds, freezing of the S^*_{CA} phase to a crystalline phase in MHPOCBC or to one of the two crystal phases (called crystal I and crystal III) in MHPOBC, occurs passing through an S^*_{IA} phase[3]. The character of the S^*_{IA}-crystal transition is catalogued as a first order and the S^*_{CA}-S^*_{IA} as a second order, or a very weak first order character.

About these subjects, the results depicted in Figure 4 indicate that a weak thermal hysteresis appears in the lowest temperature peak, since the maximum value of the peak for the 0.5, 1 and $2\,Kh^{-1}$ scan rates occurs at 320.06 K, 319.85 K and 319.78 K, respectively. As concerns the smaller peak, thermal hysteresis provides a shift in the maxima of heat capacity, less than 0.1 K, and therefore a weak first-order character can be associated with these transitions.

From the above reasons, it is possible to assign the smallest peak to the S^*_{CA}-S^*_{IA} transition and the other one to the S^*_{IA}-S^*_J transition. Since these results are not enough in order to prove the existence of the S^*_{IA} phase in our compound, X-ray measurements have been carried out.

The X-ray patterns in the low angle region, (Fig. 5), gives for the S^*_{CA} phase the usual diffraction signals corresponding to this type of phase, i.e. sharp Bragg reflection in the small angle region. This feature indicates a lamellar stacking and the wide diffuse halo

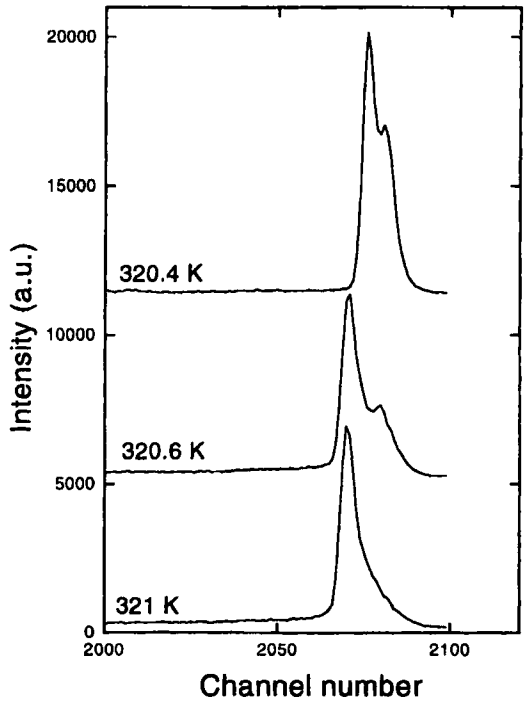

FIGURE 5 Low angle X-ray diffraction patterns at small angle region, taken as a function of decreasing temperature. At the temperature 321 K corresponds to the S^*_{CA} phase; at 320.6 K, there is coexistence between two lamellar phases (S^*_{CA} and S^*_I phases); at 320.4 K, there is coexistence between the S^*_I and S^*_J phases.

present in the wide angle region corresponds to the liquid-like arrangement of the molecules within the layers. The layer spacing determined close to the transition towards the S^*_J phase is 35.8 Å.

Half a degree lower in temperature, we observed another lamellar system where the layer spacing is 41.0 Å, together with a rather narrow (but not sharp) diffraction signal in the wide angle region, similar to the patterns already seen for a S^*_{IA} phase[14,15]. Moreover, the increase in the layer spacing observed at the transition is in agreement and in the same order of magnitude (a few Angstroms) with that observed for the same transition (S_C to S_I) reported for TBDA[16] and for the S^*_C-S^*_I reported for the related MHPOCBC[15]. In the first compound, the increase corresponds to a change in the tilt angle, however, in the MHPOCBC compound the jump in the layer spacing has been attributed to molecular conformation changes, since the tilt angle hardly changes at the S^*_{CA}-S^*_I transition. In our compound, both effects could contribute toward explaining the discontinuity in the layer thickness, but the difficulties in orienting the material during cooling have precluded its measurement. The values obtained for S^*_{CA} by electrooptic experiments during a heating process are in agreement to those reported in the literature[9].

Finally, a third lamellar stacking appeared a few tenths of a degree below, corresponding to a lamellar spacing of 38.0 Å, together with the appearance in the wide angle region of several diffraction signals, as usually observed for a crystalline S_J^* phase. These observations, not inconsistent with the other experimental results presented above, indicate that the S_{CA}^* to S_J^* phase transition passes through another phase which could be S_{IA}^*. Besides, it has to be pointed out that the transition S_{CA}^*-S_{IA}^*-S_J^* are first order, since inside the narrow temperature range where they take place, the lamellar stackings of two of these phases (S_{CA}^*-S_{IA}^* on one side, S_{IA}^* and S_J^* on the other) are simultaneously observed. This is in agreement with the fact that both transitions undergo a weak hysteresis, as observed in Cp measurements.

In Figure 6 we have represented ε' at 125 Hz in the range of interest. At 320.6 K the permittivity shows a decrease that should correspond to the transition to the monotropic S_J^* phase according to Goodby[9]. Nevertheless, at least near the S_{CA}^* phase, dechiralization lines can be observed under the polarizing microscope. In spite of textural changes not being clear, these lines disappear after a maximum of three degrees. In Figure 6, an additional change around 317.6 K can be seen that corresponds to the transition from the monotropic phase to S_J^*.

However, while the data we have obtained are not inconsistent with the presence of a monotropic S_{IA}^* phase, the data are insufficient for unequivocal identification.

3.3. S_A-S_C* Transition and Restructuring C* Phases

The S_A^*-S_C^* transition is shown in Figure 7. The data have been obtained on heating the sample at a rate of 1 Kh^{-1}. The transition appears at 376.50 K, in agreement with the

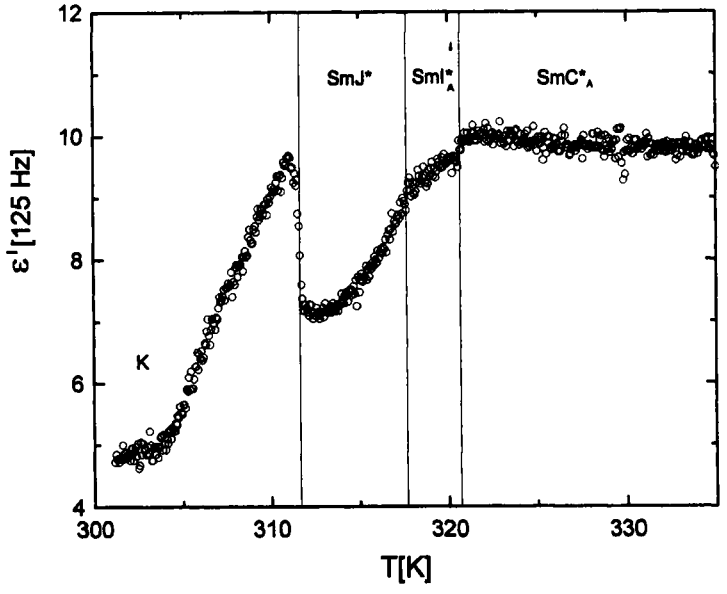

FIGURE 6 Dielectric permittivity constant, ε', versus temperature, measured at a frequency of 125 Hz and with a cooling rate of 1 K/min.

transition temperature of the tiny peak detected by DSC at a temperature rate 10^2-10^3 times faster than our scan rates. Its analysis was carried out using the extended Landau model, due to the lack of appreciable excess heat capacity about T_c. In that model, the free energy of the S_C^* phase relative to that of the S_A phase is expanded as a function of the tilt angle order parameter, θ, by the expression

$$G = a\,t\,\theta^2 + b\,\theta^4 + c\,\theta^6 \tag{1}$$

where $t = (T - T_c)/T_c$ is the reduced temperature. The signs of the a and c coefficients are positive, while $b > 0$ if the transition is second order and $b < 0$ for a first order character.

In this approach, the anomalous heat capacity for temperatures $T < T_c$ can be written as

$$C_p = A\,T(T_k - T_c)^{1/2}/T_c(T_k - T)^{1/2} \tag{2}$$

where $T_k = T_c(1 + b^2/3ac)$ is the metastability limit and A is the value of the discontinuity in C_p at T_c. When we are approaching a tricritical point, though in the second order line transition, the b coefficient tends towards 0 and subsequently $T_k \to T_c$.

In order to obtain the experimental C_p to the S_A-S_J^* transition, we substract a linear background from the total specific heat (sample plus addenda). This baseline is deduced by linearly fitting the C_p data in the temperature range 378 K < T < 381 K and

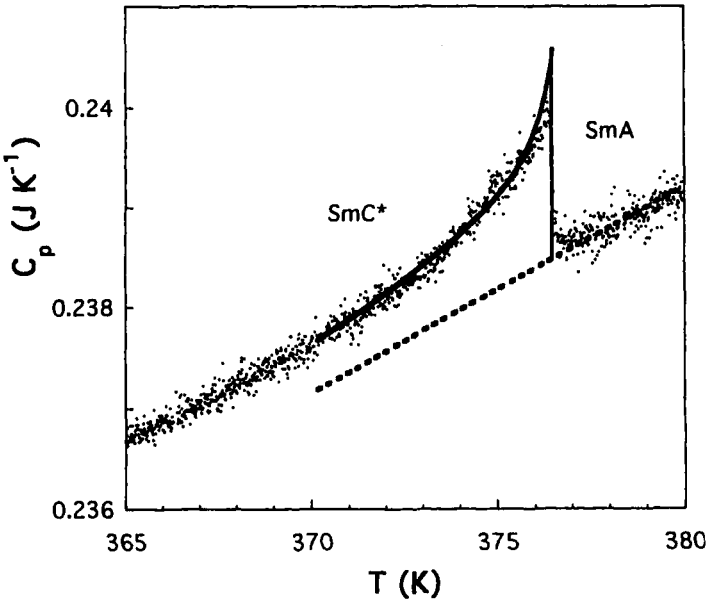

FIGURE 7 Heat capacity at the transition S_A-S_C^* obtained with a cooling rate of 1 Kh^{-1}. Solid lines are fits to the theoretical predictions of the Landau model. Dashed lines represent the estimated Cp background for obtaining the anomalous heat capacity in this transition.

extrapolated to the lower temperatures, but still around T_c. This fitted region is such that we avoid the possible non-Landau C_p tail existing just above T_c, which could be associated with pre-transitional fluctuations or inhomogeneities due to impurities. Figure 7 shows the calculated baseline and the best theoretical Landau fit.

The Landau fitting parameters are given in Table I. The value of T_c corresponds to the temperature where C_p gets the midvalue of the total jump. The quantity δH is defined $\delta H = \int_0^{Tc} C_p dT$ where C_p is the excess heat capacity given by equation (2). A difference appears between the calculated $\delta H = 1.37\ \mathrm{Jg}^{-1}$ and the $0.74\ \mathrm{Jg}^{-1}$ value obtained by our DSC measurements. This is due, in part, to the more extended, anomalous C_p region for the theoretical calculations and the difficulties in distinguishing the C_p excess contributions from the baseline in the DSC thermogramms. Table I also shows the values of some Landau fits for the S_A-S_C^* transition in the MHPOBC and MHPOCBC related compound.

As far as the quantity $t_0 = 3(T_k - T_c)/T_c$ is concerned, which determines the full width at half height of the C_p peak maximum, our compound presents a larger value than that for related chiral compounds. However, this value lies in the middle of the range from 6.5×10^{-3} to 0.8×10^{-3} reported for the S_A-S_C transition in other non-polar and non-chiral compounds[17]. In order to compare the jump of C_p at the transition with other compounds, we use the quantity $A_R = AM/R$, where M is the molecular weight ($M = 586.824\ \mathrm{g\ mol}^{-1}$). Our compound presents a higher peak than the MHPOCBC, but smaller than MHPOCBC compound. Both quantities, t_0 and A_R, allow us to consider that the behavior of MHDOBBC is as the non-chiral 8S5 compound, where $A_R = 5$ and $t_0 = 6.5 \times 10^{-3}$.[18]. Therefore, it means that the correlation between the Landau fit parameters and the chiral character of the molecules cannot be established. Since the transition temperature in MHDOBBC is practically uninfluenced by the enantiomeric purity (378.5 K for the S compound and 378.0 for the R)[9], we could consider that the transition is driven by structural features more than by dipolar interactions.

As fas as restructuring phases is concerned, recent work on this compound using dielectric spectroscopy[17] has given a different phase sequence, since a new phase appears during a temperature range of one degree between the S_A and S_C^* phase: the $S_{C\alpha}^*$ phase. Therefore, what we have mentioned above as S_A-S_C^* should be S_A-$S_{C\alpha}^*$. On cooling from the isotropic phase at $-2\ \mathrm{Kh}^{-1}$, and below the S_A-$S_{C\alpha}^*$ transition, our C_p data show an absence of defined peaks. It is in agreement with the idea that these kinds of phase transitions are not detected by ac calorimetry, as we have previously mentioned in the introduction about MHPOBC. This is due to the transitions between

TABLE I

Landau parameters for fitting the S_A-S_C^* transition with equation (2). The enthalpy value corresponds to the integrated theoretical heat capacity. Data of MHPOBC and MHPOCBC compounds are listed to compare [3].

System	T_c(K)	T_k(K)	A_R	$10^3 t_0$	δH(Jg^{-1})	Ref
This Compound	376.50	376.88	6.3	3.03	1.39	Our work
MHPOBC	395.92	396.17	16.3	1.92	3.10	[3]
MHPOCBC	378.50	378.71	3.0	1.65	0.48	[3]

the restructuring phases having a first-order character, with very small latent heats, associated with the physical rearrangement between layers, while the ordering within each layer remains unchanged.

However, our results present two very small rounded anomalies, centred around 352 K and 343 K, with a size close to the resolution limit, but without any explanation from an external experimental reason. The highest temperature shoulder coincides with the ferro-ferri temperature transition. The other shoulder appears at temperatures around the $S^*_{C\gamma}$-S^*_{CA} transition according to the transitions given by Goodby.[3] Our DSC measurements at 20 K min^{-1} also clearly show a small peak at 347 K with a width of 3 K, which is the region of the $S^*_{C\gamma}$-S^*_{CA} transition.

4. CONCLUSIONS

The different phases of the antiferroelectric MHDOBBC compound have been studied with high resolution ac calorimetry. The implemented "thermistor method", as an alternative to the shift phase method, has allowed the detection of strong pre-transitional effects in the melting transition and the observation that the S^*_{CA} phase is a long, metastable phase. Two monotropic phases appear in the freezing process of the S^*_{CA} which were studied by X-rays, dielectric and optical measurements. The lower of the two phases is S^*_J, but the upper phase resisted unequivocal characterization. The S_A-$S^*_{C\alpha}$ has been clearly detected and it was well described by the usual extended Landau model. A comparison with other related compounds has been performed in order to obtain a correlation between the Landau fit parameters and the corresponding molecular behaviour. The restructuring phases between S_A and S^*_{CA} are not detected by ac calorimetry and DSC, although an anomalous thermal behaviour appears close to the $S^*_{A\gamma}$-S^*_{CA} transition.

Acknowledgements

This work was supported by CICYT (Spain). Projects: MAT94-0325-E, MAT94-0717-CO2-2 and the project 79B-TM of Spain-France actions.

References

1. A. Fukuda, Y. Takanishi, T. Isozaki, K. Ishikawa, H. Takezoe, *J. Mater. Chem.* **4**, 997 (1994).
2. D. L. Chandani, Y. Ouchi, H. Takezoe, A. Fukuda, K. Terashima, K. Furukawa, A. Kishi, *Jpn. J. Appl. Phys.*, **28**, L1261 (1989).
3. K. Ema, H. Yao, I. Kawamura, T. Chan, C. W. Garland, *Phys. Rev. E*, **47**, 1203 (1993).
4. S. Asahina, M. Sorai, A. Fukuda, H. Takezoe, K. Furukawa, K. Terashima, Y. Suzuki, I. Kawamura, *Abst. 4th Int. Conf. on FLCs* (Tokyo), **147** (1993).
5. K. H. Kim, Y. Takanishi, K. Ishikawa, H. Takezoe, A. Fukuda, *Liq. Crys.*, **16** 187 (1994).
6. M. Neundorf, S. Diele, S. Ernst, S. Saito, D. Demus, T. Inukai, K. Murashiro, *Ferroelectric*, **147**, 95 (1993).
7. J. A. Puértolas, M. Castro, M. R. de la Fuente, M. A. Perez Jubindo, M. Cano, M. B. Ros, *Proc. Int. Conf. on Liq. Cryst.* (Budapest) **1**, 244 (1994).
8. S. Hiller, S. A. Pkin, J. W. Goodby, I. Nishiyama, W. Haas, *Proc. Int. Conf. on Liq. Cryst.* (Budapest) **2**, 859 (1994).
9. J. W. Goodby, J. S. Patel, E. Chin, *J. Mater. Chem.*, **2**, 197 (1992).
10. M. Castro, J. A. Puértolas, *J. Therm. Analys.*, **41**, 1245 (1994).

11. M. Castro, Phd. Thesis. Zaragoza University (Spain) (1995).
12. M. A. Pérez Jubindo, A. Ezcurra, J. Etxebarra, A. Remón, M. J. Tello, *Mol. Cryst. Liq. Cryst.*, **159**, 137 (1988).
13. K. J. Lushington, G. B. Kasting, C. W. Garland, *J. Phys. Lett.* (Paris), **41**, L419 (1980).
14. J. J. Benattar, *Phd. Thesis.* Paris-Sud. University (France) (1989).
15. Y. Takanishi, H. Takezoe, A. Fukuda, *Ferroelectric*, **147**, 135 (1993).
16. D. Guillon, A. Skoulios, J. J. Benattar, *J. Phys.* France, **47**, 133 (1986).
17. M. R. De la Fuente, S. Merino, Y. González, M. A. Perez Jubindo, B, Ros, J. A. Puertolas, M. Castro, *Adv. Matter*, **7**, 564 (1995).
18. C. C. Huang, J. M. Viner, *Phys. Rev. A*, **25**, 3385 (1982); M. Meichle, C. W. Garland, *Phys. Rev.*, **27**, 2624 (1983).
19. O. Mitsunbu, *Synthesis*, **1**, 1 (1981).
20. Y. Gonzalez. *Phd. Thesis.* Zaragoza University (1995).